Differential Distribution of cAMP-Specific Phosphodiesterase 7A mRNA in Rat Brain and Peripheral Organs

X. MIRÓ,[1] S. PÉREZ-TORRES,[2] J.M. PALACIOS,[†] P. PUIGDOMÈNECH,[1] AND G. MENGOD[2*]
[1]*Department of Molecular Genetics, Instituto de Biología Molecular de Barcelona, CID-CSIC, Barcelona, Spain*
[2]*Department of Neurochemistry, Instituto de Investigaciones Biomédicas de Barcelona, CSIC-IDIBAPS, Barcelona, Spain*

KEY WORDS in situ hybridization; area postrema; white matter; RT-PCR; splice variants

ABSTRACT We investigated the regional distribution and cellular localization of mRNA coding for the cAMP-specific phosphodiesterase 7A (PDE7A) in rat brain and several peripheral organs by in situ hybridization histochemistry. The regional expression of two splice variants, PDE7A1 and PDE7A2, was examined by RT-PCR using RNA extracted from several brain regions. PDE7A mRNA was found to be widely distributed in rat brain in both neuronal and nonneuronal cell populations. The highest levels of hybridization were observed in the olfactory bulb, olfactory tubercle, hippocampus, cerebellum, medial habenula nucleus, pineal gland, area postrema, and choroid plexus. Positive hybridization signals were also detected in other areas, such as raphe nuclei, temporal and entorhinal cortex, pontine nuclei, and some cranial nerve motor nuclei. Both mRNA splice forms were differentially distributed in several areas of the brain with the striatum expressing only PDE7A1 and the olfactory bulb and spinal cord expressing PDE7A2 exclusively. In peripheral organs the highest levels of PDE7A hybridization were seen in kidney medulla, although testis, liver, adrenal glands, thymus, and spleen also presented high hybridization signal. These results are consistent with PDE7A being involved in the regulation of cAMP signaling in many brain functions. The consistent colocalization with PDE4 mRNAs suggests that PDE7A could have an effect on memory, depression, and emesis. The results offer clear anatomical and functional systems in which to investigate future specific PDE7 inhibitors. **Synapse 40:201–214, 2001.**

INTRODUCTION

Cyclic AMP (cAMP) plays a key role in signal transduction in a wide variety of cellular responses such as gene transcription (Lalli and Sassone-Corsi, 1994), activation of ion channels (Goulding et al., 1994; Zagotta and Siegelbaum, 1996), neurotransmitter biosynthesis (Kaufman, 1995) and release (Kandel and Schwartz, 1982), survival of dopaminergic neurons (Yamashita et al., 1997), synaptic facilitation and potentiation (Zhong and Wu, 1991), and as a response regulator (Morimoto and Koshland, 1991). cAMP is synthesized by the enzyme adenylyl cyclase (Houslay and Milligan, 1997). However, the only mechanism for its degradation is through the action of cyclic nucleotide phosphodiesterases (PDEs), which catalyze the hydrolysis of 3′,5′-cyclic nucleotides into 5′-nucleoside monophosphates. PDEs have so far been classified into at least 11 families, based on their substrate specificity, cofactor requirement, and selective inhibition by different compounds (Conti and Jin, 1999; Fawcett et al., 2000). They have different regulatory properties and intracellular location, with particular isoforms being expressed in a cell-specific fashion (Conti and Jin, 1999). Families 4, 7, and 8 specifically hydrolyze cAMP, with PDE7 and PDE8 having a higher affinity for this substrate. The PDE4 family is the largest described, with at least four different genes (PDE4A, PDE4B, PDE4C, and PDE4D) (Houslay et al., 1998) each one expressing several splice variants. Two members of each of the PDE7 and PDE8 families have been cloned, PDE7A (Michaeli et al., 1993; Soderling et al., 1998), PDE7B (Hetman et al., 2000; Sasaki et al., 2000), and PDE8A (Fisher et al.,

*Correspondence to: Guadalupe Mengod, Department of Neurochemistry, Instituto de Investigaciones Biomédicas de Barcelona, CSIC-IDIBAPS. c/ Rosselló 161, 6ª. E-08036 Barcelona, Spain. E-mail: gmlnqr@iibb.csic.es

[†]Permanent address: Research Center, Almirall Prodesfarma S.A., Barcelona, Spain.

Received 7 July 2000; Accepted 21 November

TABLE I. PDE7A mRNA Distribution in rat brain

Brain area	PDE7A	Brain area	PDE7A
Cortex		Ventromedial hypothalamus	+
Parietal cortex		Dorsomedial hypothalamic nucleus	+
layer II, III	++	Pineal gland	+++
layer IV	+++	Brainstem	
layer V	++	Raphe nuclei	
layer VI	++	dorsal	+/++
Frontal cortex	++	median	+
Cingulate cortex	++	magnus	+
Retrospenial cortex	+/++	pallidus	−/+
Entorhinal cortex	++	obscurus	−
Olfactory system		Red nucleus	++
Olfactory bulb	+++	Principal oculomotor nerve	++
Anterior olfactory nucleus	++	Superior colliculus	+/++
Olfactory tubercle	++	Pontine nucleus	++/+++
Piriform cortex	+++	Parabigeminal nucleus	+/++
Islands of Calleja	+/++	Reticulotegmental nucleus pons	+/++
Islands of Calleja, major island	+/++	Nucleus of the spinal tract of the trigeminus	+/++
Sub, ependyma layer and olfactory ventricle	+/++	Vestibular nuclei	+/++
Basal ganglia and related areas		Hypoglossal nucleus	++
Caudate-Putamen	++	Prepositus hypoglossal nucleus	+/++
Accumbens	−	Lateroreticular nucleus	+
Ventral pallidum	+	Accessory facial nucleus	++
Substantia nigra		Facial nucleus	+
pars compacta	++	Nucleus of the solitary tract	+/++
pars reticulata	++	Inferior olive	+/++
Limbic areas		Cuneate nuclei	++
Ammon's horn		Area postrema	+
CA1 (pyramidal cell layer)	++	Dorsal cochlear nuclei	+/++
CA2 (pyramidal cell layer)	++/+++	Gracile nucleus	++
CA3 (pyramidal cell layer)	++/+++	Ventral tegmental nucleus	++
CA4 (pyramidal cell layer)	++/+++	Sensory root trigeminal nerve	+
Dentate gyrus	+++	Principal sensory trigeminal nerve	+
Induseum griseum	+/++	Kölliker-Fuse nucleus	+
Subiculum	++	Dorsal motor nucleus of vagus	
Pre, parasubiculum	++	Cerebellum	
Amygdala	++	Molecular layer	−
Lateral septal nucleus	+	Granular layer	++/+++
Medial septal nucleus	+	Purkinje cell layer	+++
Thalamus and Hypothalamus		White matter	−
Medial habenular nucleus	++/+++	Cerebellar nuclei	+
Lateral habenular nucleus	+/++	Nonneuronal structures	
Ventroposterior thalamic nuclei	+/++	Interpeduncular nuclei	+/++
Laterodorsal thalamic nucleus	+/++	Cerebral peduncle	+/++
Mediodorsal thalamic nucleus	+/++	Middle cerebellar peduncle	+
Reticular thalamic nucleus	+	Choroid plexus	++/+++
Medial geniculate nucleus	+/++	Aqueduct	+
Zona incerta	++	Lateral ventricle	++
Internal capsule	+/++		

The levels of expression are indicated by "+" for low hybridization signal up to "+++" for highest hybridization signal; "−" not detected.

1998) and PDE8B (Hayashi et al., 1998), respectively. PDE4 isozymes are characterized by their specific sensitivity to rolipram, a selective PDE4 inhibitor, and are found differentially distributed in the rat brain (Cherry and Davis, 1999; Pérez-Torres et al., 2001). There is scarce information about the distribution PDE7 and PDE8 transcripts in the central nervous system, but both mRNAs have been detected in mouse brain by Northern blot analysis (Bloom and Beavo, 1996; Soderling et al., 1998) and in human and rat tissues by RT-PCR (Hoffman et al., 1998). Additionally, PDE7A mRNA has been visualized by in situ hybridization in a few adult and embryonic rat brain regions in a preliminary study (Hoffman et al., 1998). More recently it has been shown that PDE7A is also expressed in the immune system and can participate in the regulation of T-cell activation (Li et al., 1999). The identification of selective PDE7 inhibitors (Martínez et al., 2000) could represent a new strategy to treat T-cell-related diseases.

Selective inhibitors of cAMP-specific PDEs have been suggested as therapies for the treatment of several human diseases, predominantly disorders of the immune and inflammatory systems (Teixeira et al., 1997) or disorders of the central nervous system such as depression (Houslay et al., 1998), multiple sclerosis (Genain et al., 1995), ischemia-reperfusion injury (Kato et al., 1995), and Alzheimer's (McGeer and McGeer, 1995) and Parkinson's diseases (Hulley et al., 1995). In particular, PDE4 inhibitors such as rolipram have been used in humans for the treatment of some of the above diseases (Genain et al., 1995). However, the extensive side effects associated with the use of PDE4 inhibitors (nausea, vomiting, and increased gastric acid secretion) (Horowski and Sastre-y-Hernandez, 1985) have prevented their widespread therapeutic use. These side

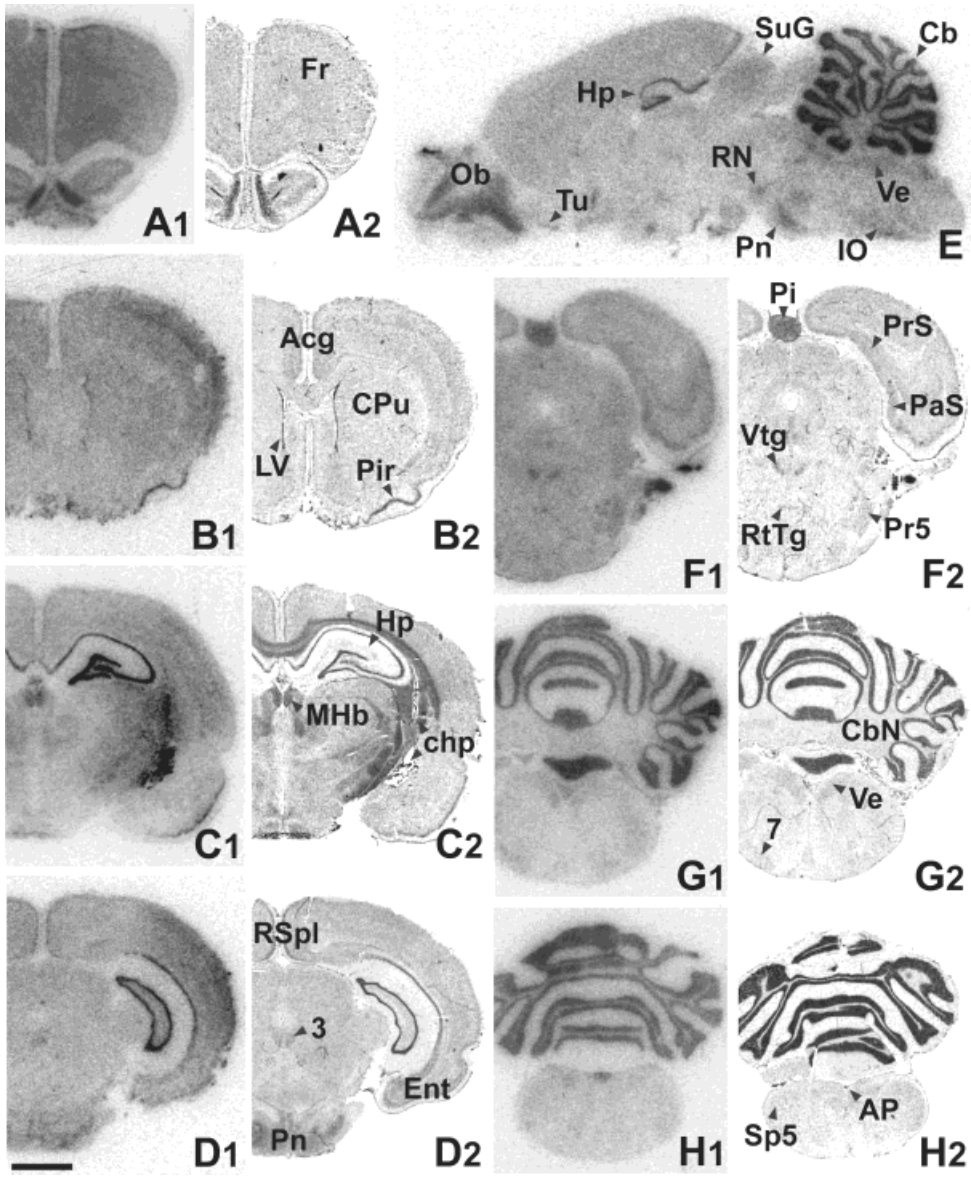

Fig. 1. Regional distribution of PDE7A mRNA in the rat brain. **A1–H1**: Film autoradiograms showing hybridization patterns with the ^{32}P-labeled oligonucleotide rPDE7A. **A2–H2**: The same hybridized slides stained with cresyl violet. Coronal brain sections are presented from **A** to **H** in a rostrocaudal progression, but **E** being a sagittal brain section. Bar = 4 mm. Anterior cingulate cortex (Acg), area postrema (AP), cerebellum (Cb), cerebellar nuclei (CbN), choroid plexus (chp), caudate-putamen (CPu), entorhinal cortex (Ent), frontal cortex (Fr), hippocampal formation (Hp), inferior olive (IO), lateral ventricle (LV), medial habenular nucleus (MHb), olfactory bulb (Ob), parasubiculum (PaS), pineal gland (Pi), piriform cortex (Pir), pontine nuclei (Pn), presubiculum (Prs), principal sensory trigeminal nerve (Pr5), red nucleus (RN), retrospenial cortex (RSpl), reticulotegmental nucleus pons (RtTg), nucleus of the spinal tract of the trigeminus (Sp5), superficial gray layer of superior colliculus (SuG), olfactory tubercle (Tu), vestibular nuclei (Ve), ventral tegmental nucleus (Vtg), principal oculomotor nerve (3), facial nucleus (7).

effects are perhaps attributable to their low selectivity for the different PDE4 isoforms. The diversity of this large superfamily of enzymes provides an array of different targets for the control of the cellular signaling processes in which they are involved and make PDEs very promising targets for the pharmacology of diseases in which modulation of cyclic-nucleotide signaling could play a pivotal role.

An important step for understanding the regulation of cyclic nucleotides in normal and disease states is the identification of the sites of synthesis of the entire PDE superfamily. In the present article we examine the regional and cellular distribution of the mRNA coding for PDE7A in the adult rat brain as well as in some peripheral organs using in situ hybridization histochemistry. Our study reveals that PDE7A mRNA has a widespread distribution in both neuronal and nonneuronal cell populations. We have also studied by RT-PCR the differential distribution of the two known PDE7A mRNA splice variants, PDE7A1 and PDE7A2, in RNA extracted from several rat brain regions.

MATERIALS AND METHODS

Tissue preparation

Adult male Wistar rats (200–300g) were purchased from Iffa Credo (Lyon, France). Animal care followed the Spanish legislation on "Protection of animals used in experimental and other scientific purposes" in agreement with the European (E.E.C) regulations (O.J. of E.C. L358/1 18/12/1986). The animals were killed by decapitation. The brains were frozen on dry ice and kept at -20°C. Tissue sections, 14 μm thick, were cut on a microtome-cryostat (Microm HM500 OM, Walldorf, Germany), thaw-mounted onto APTS (3-aminopropyltriethoxysilane; Sigma, St. Louis, MO) coated slides, and kept at −20°C until used.

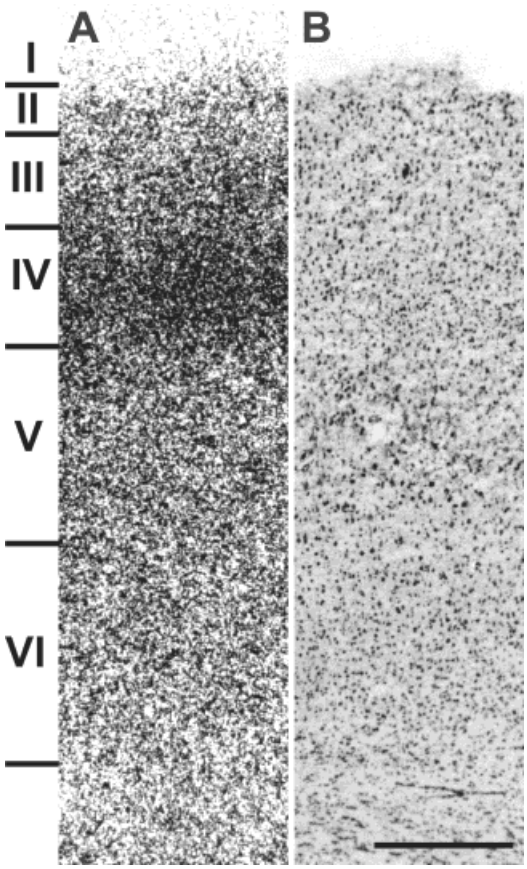

Fig. 2. Distribution of PDE7A mRNA in the neocortex. Note the enrichment of the hybridization signal in layer IV (**A**). **B**: The same field from a consecutive section stained with cresyl violet. Bar = 0.5 mm.

In situ hybridization histochemistry

A 45-base oligodeoxyribonucleotide complementary to the common amino region for the isoforms PDE7A1 and PDE7A2 was used as a hybridization probe to detect PDE7A mRNA. This region was chosen because it shares no similarity with other members of the different PDE families. The oligodeoxyribonucleotide used (rPDE7A) was complementary to bases 238–194 (Acc. no. U68171) and was synthesized by Pharmacia Biotech (Little Chalfont, UK).

The oligonucleotide was labeled at its 3′-end using [α-^{32}P]dATP (3000 Ci/mmol, New England Nuclear, Boston, MA) and terminal deoxynucleotidyltransferase (TdT, Roche Molecular Biochemicals, Mannheim, Germany). The labeling reaction, purification of the probe, tissue treatment before hybridization, and hybridization procedures were carried out as described by Tomiyama et al. (1997). Autoradiograms were generated by apposing the hybridized tissue sections to βmax films (Amersham, Buckinghamshire, UK) for 4 weeks at -70°C with an intensifying screen.

The specificity of the autoradiographic signal obtained in the in situ hybridization experiments was verified with a series of routine controls. The addition in the hybridization solution of a 50-fold excess of the same unlabeled oligonucleotide resulted in the complete abolition of the specific hybridization signal; the remaining signal was considered to be the background level. The thermal stability of the hybrids was examined by washing at increasing temperatures: a sharp decrease in the hybridization signal was observed at a temperature consistent with the T_m of the hybrids

Duplicates of the hybridized sections were dipped in autoradiographic emulsion, Hypercoat LM-1 emulsion (Amersham). The emulsion was developed after 6 weeks exposure at 4°C in Kodak D19. Sections were examined using bright- and dark-field light microscopy (Leitz, Laborlux S, Wetzlar, Germany). For anatomical reference, sections close to those used were stained with cresyl violet.

Reverse transcriptase-polymerase chain reaction amplification

Oligonucleotide primers used for PCR amplification of PDE7A splice variants A1 and A2 were designed according to the published sequences. Oligonucleotides were as follows: PDE7AR1 (944-924, Acc. no. U77880), PDE7A1F (32-53, Acc. no. L12052), PDE7A2F (89-111, Acc. no. U68171), PDE7AF1 (139-161, Acc. no. U68171), PDE7AR2 (706-685, Acc. no. U77880).

Total RNA from Jurkat cells and selected rat brain regions was isolated by the acid guanidinium thiocyanate-phenol-chloroform extraction technique (Chomczynski and Sacchi, 1987) and treated with RNase-free DNase (Roche Molecular Biochemicals). RNA (5 μg total) was reverse-transcribed into cDNA using standard protocols with PDE7AR1. The PCR amplifications were performed with the oligonucleotide PDE7AR1 and the specific oligonucleotides for PDE7A1 (PDE7A1F) or PDE7A2 (PDE7A2F) (30 sec at 94°C, 30 sec at 70°C, and 90 sec at 72°C for 35 cycles). Then a nested PCR amplification was developed with the oligonucleotides PDE7AF1 and PDE7AR2 using 1% of the volume of the previous PCR reaction products (30 sec at 94°C, 30 sec at 70°C, 70 sec at 72°C for 30 cycles). All PCR-derived fragments were electrophoretically separated on a 1.5% Tris/borate/EDTA agarose gel. The electrophoresed DNA was transferred to a nylon membrane (Nytran) and hybridized with the PDE7A-specific ^{32}P-labeled oligonucleotide probe rPDE7A to confirm the identity of all PCR amplified bands (data not shown).

Fig. 3. Localization of PDE7A mRNA in cells of the anterior olfactory nucleus (**A**), different layers of the olfactory bulb (**B**), piriform cortex (**C**), major island of Calleja (D), olfactory tubercle and islands of Calleja (**E**). **A1–E1**: Photomicrographs from emulsion autoradiogram, obtained with dark-field illumination. Autoradiographic grains are seen as bright points. **A2–E2**: Bright-field photomicrographs from the same sections stained with cresyl violet. Asterisk indicates tissue light. Bar = 0.4 mm (**A**) and 0.1 mm (**B–E**). Intrabulbar part of the anterior commissure (aci), dorsal (AOD), lateral (AOL), medial (AOM) and ventral (AOV) anterior olfactory nuclei, ependymal layer (E), ependymal and subependymal layer of the olfactory ventricle (E/OV), external plexiform layer (EPL), glomerular layer (Gl), islands of Calleja (ICj), major island of Calleja (ICjM), internal granule cell layer (IGr), mitral cell layer (Mtr), piriform cortex (Pir), olfactory tubercle (Tu).

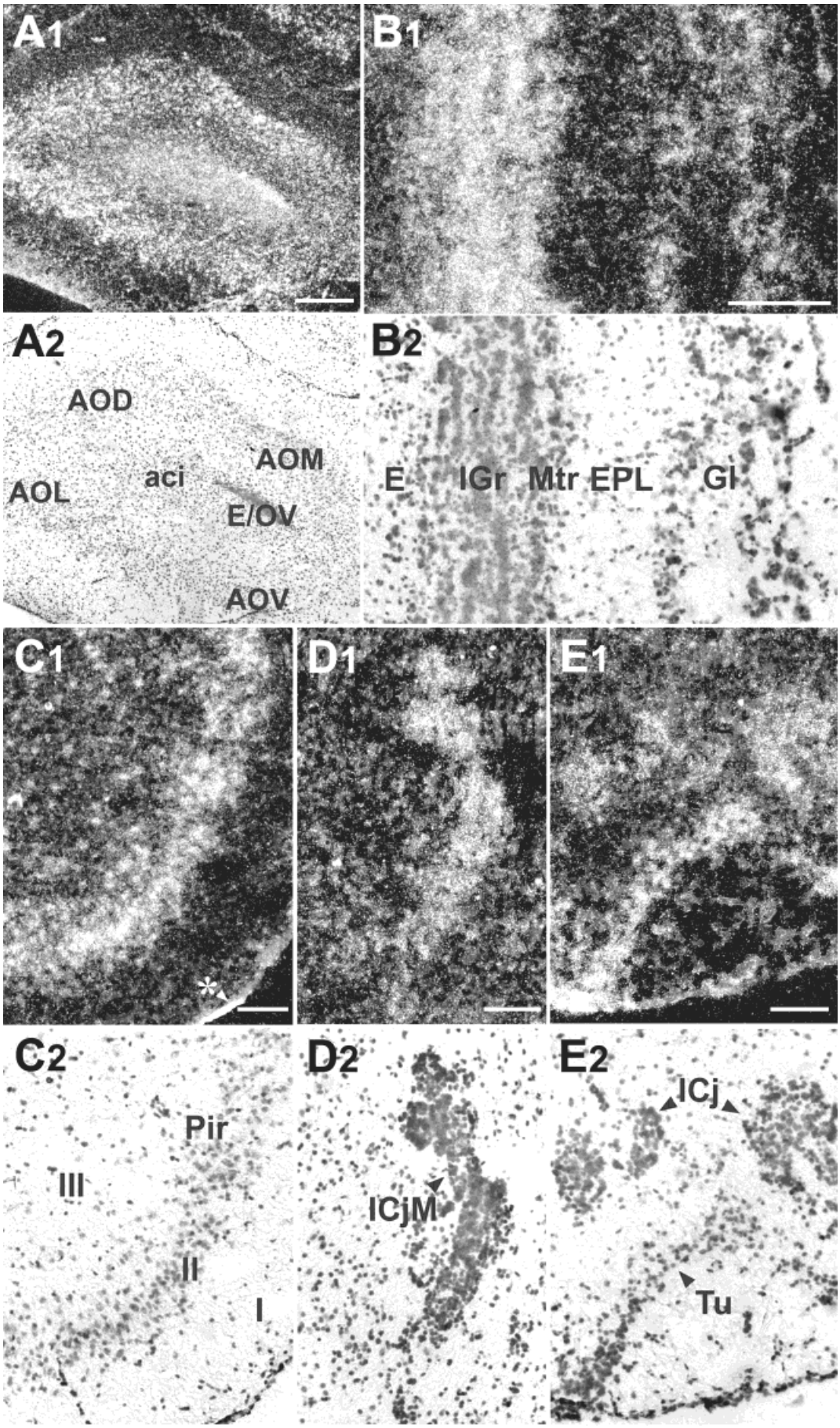
A1
B1
A2
AOD
AOM
aci
AOL
E/OV
AOV
B2
E
IGr
Mtr
EPL
Gl
C1
D1
E1
*
C2
Pir
III
II
I
D2
ICjM
E2
ICj
Tu

Fig. 3

RESULTS

The distribution of the PDE7A mRNA visualized by in situ hybridization histochemistry in the rat brain (summarized in Table I) and in peripheral organs showed a heterogeneous pattern. Labeled brain nuclei were identified by comparison of the film autoradiograms both with cresyl violet staining of the hybridized tissues and acetylcholinesterase activity of neighboring sections. The highest levels of expression in the brain were found in the hippocampus, cerebellum, pineal gland, and olfactory bulb. In peripheral organs the highest levels were observed in thymus, kidney, and testis.

Cortex

PDE7A mRNA was observed in different areas of the cortex (Fig. 1). A homogeneous hybridization pattern of intermediate intensity could be observed in frontal cortex (Fig. 1A1) and in cingulate cortex (Fig. 1B1,C1). In the retrospenial cortex (Fig. 1D1) labeled cells were concentrated in layer II-III, whereas scattered hybridizing cells could be seen throughout the rest of the layers. The parietal cortex (Fig. 1B1) presented high hybridization levels in all layers, being especially high in layer IV (Fig. 2A). In the entorhinal cortex, the strongest hybridization signal could be observed in large stellate cells of layer II, while weak hybridization levels could be seen in cells scattered throughout the rest of the layers (Fig. 1D1).

Olfactory system

The mRNA encoding PDE7A was abundant in the olfactory bulb (Fig 1E). The strongest hybridization signal was found in the internal granule cell layer and the mitral cell layer and the interneurons of the glomerular layer (Fig. 3B1). Moderate levels of PDE7A mRNA were detected in the medium-sized tufted cells of the external plexiform layer. In the anterior olfactory nucleus (Figs. 1A, 3A1) high levels of PDE7A mRNA were detected in the dorsal and lateral nuclei. The ependyma and subependyma layer and olfactory ventricle were enriched in PDE7A mRNA (Figs. 1A1, 3A1).

In the olfactory tubercle, PDE7A mRNA was present in many scattered, very intensely labeled cells, both in the pyramidal cell layer and polymorph cell layer (Figs. 1B1,E, 3E1) some associated with the cell clusters of the islands of Calleja (Fig. 3E1), including the insula magna (Fig. 3D1). In the piriform cortex the strongest hybridization signal was observed in cells from layer II (Fig. 3C1).

Basal ganglia and related areas

A moderate hybridization signal for PDE7A mRNA was observed in caudate-putamen (Fig. 1B1). The substantia nigra pars reticulata and the pars compacta presented intermediate levels of PDE7A mRNA (Fig. 5C1).

Limbic areas

The hippocampal formation presented very high hybridization signals of PDE7A mRNA (Fig. 1C1,E, 4B1). Very strong hybridization signals were also seen in the granule cell layer of the dentate gyrus and the pyramidal cell layer of Ammon's horn, particularly in the CA3 field. The subiculum, presubiculum, and parasubiculum showed intermediate levels of PDE7A mRNA (Fig. 1F1). A low hybridization signal was detected in the lateral and medial septal nuclei (Fig. 1B1). Few strongly labeled cells were seen in the indusium griseum (Fig. 4E). Intermediate to low hybridization signals were detected in some amygdaloid nuclei (Fig. 5E).

Thalamus and hypothalamus

PDE7A transcripts were present at intermediate levels in the lateral and medial ventroposterior thalamic nuclei as well as in the laterodorsal, reticular, and mediodorsal thalamic nuclei (Fig. 1C).

High hybridization levels were observed in the medial habenular nucleus, whereas moderate levels of expression were seen in the lateral habenular nucleus (Fig. 1C). Low hybridization signals were present in the medial geniculate nucleus (Figs. 1D, 4C). A strong hybridization signal was detected in the pineal gland (Fig. 1F). In the hypothalamus, moderate PDE7A mRNA levels were detected in the ventromedial hypothalamus and in the compact area of the dorsomedial hypothalamic nucleus (Fig. 1C).

Brainstem

The pontine nuclei showed high levels of hybridization signal (Fig. 1D,E). Other midbrain structures presenting intermediate to low levels of hybridization signals included the superior colliculus, particularly the superficial gray layers (Figs. 1E,F, 5A), the reticulotegmental nucleus of the pons (Fig. 1F), the parabigeminal nucleus and the red nucleus (Figs. 1E, 4D).

Certain raphe nuclei showed low hybridization signals. These include the dorsal raphe nucleus (Fig. 6A), median raphe nucleus (Fig. 6B), and the raphe magnus nucleus (Fig. 6C). A clear hybridization signal could be seen in the raphe pallidus (Fig. 6C), in contrast with its absence in the raphe obscurus. A clear hybridization signal was observed in the ventral tegmental nucleus (Fig. 1F).

Fig. 4. Distribution of PDE7A mRNA in cells of the choroid plexus (**A**), hippocampal formation (**B**), dorsal part of the medial geniculate nucleus (**C**), red nucleus (**D**), and induseum griseum (**E**). **A1–E1**: Dark-field photomicrographs from emulsion dipped sections. **A2–E2**: Bright-field photomicrographs from the same sections stained with cresyl violet. Asterisk in **E1** indicates tissue light in the cerebral longitudinal fissure. Bar = 0.2 mm (**B**) and 0.1 mm (**A,C–E**). Brachium of the superior colliculus (bsc), fields one (CA1) and four (CA4) of Ammon's horn, corpus callosum (cc), dentate gyrus (DG), induseum griseum (IG), stratum lacunosum moleculare of Ammon's horn (LMol), dorsal part of the medial geniculate nucleus (MGD), molecular layer of the dentate gyrus (Mol), marginal zone of the medial geniculate (MZMG), stratum radiatum of Ammon's horn (Rad).

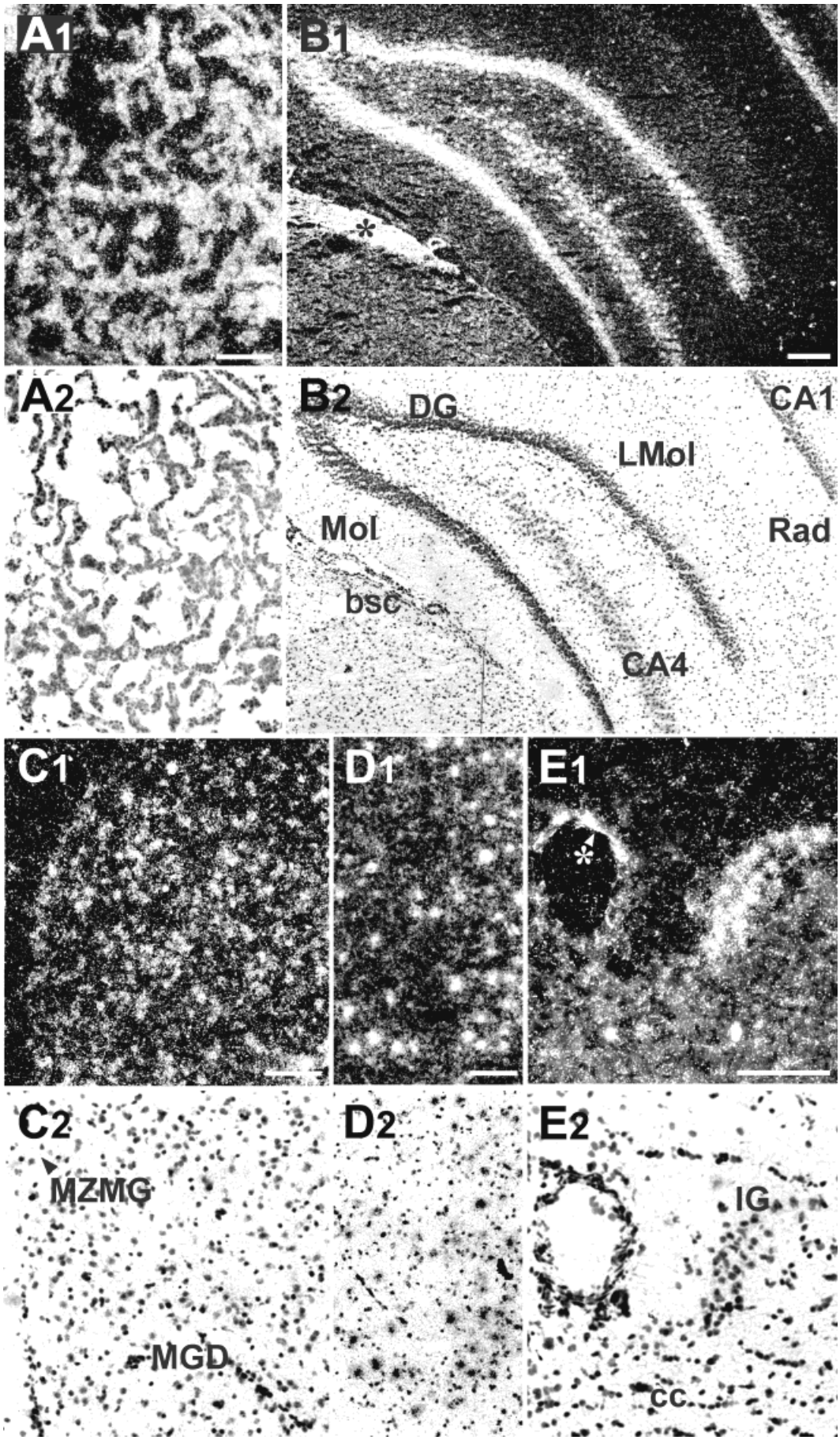
A1
B1
A2
B2
DG
CA1
LMol
Mol
Rad
bsc
CA4
C1
D1
E1
C2
D2
E2
MZMG
IG
MGD
cc

Fig. 4

Hybridization signal for PDE7A mRNA could be observed in the principal oculomotor nerve (Fig. 1D), hypoglossal nucleus (Fig. 7E), facial nucleus (Fig. 1G), nucleus of the spinal tract of the trigeminus (Fig. 1H), sensory root of the trigeminal nerve (Fig. 1F), principal sensory trigeminal nerve (Fig. 1F), the dorsal motor nucleus of vagus (Fig. 7D), and accessory facial nucleus. Intermediate levels of hybridization were seen in the vestibular nuclei (Fig. 1E,G), prepositus hypoglossal nucleus, nucleus of solitary tract (Fig. 5E), and dorsal cochlear nuclei (Fig. 1G). Moderate hybridization signals were observed in the area postrema (Figs. 1H, 7B), gracile (Fig. 7A), and cuneate nuclei (Fig. 7C). Labeled cells were also detected in the lateral reticular nucleus (Fig. 7F) and in the inferior olive (Fig. 1E).

Cerebellum

One of the highest hybridization signals for PDE7A mRNA in rat brain was observed in Purkinje cells and in granular layer (Fig. 6D) of cerebellum (Fig. 1E). Low levels of expression were observed in the deep cerebellar nuclei (Fig. 1G).

Nonneuronal structures

Low levels of hybridization signal for PDE7A mRNA were observed in white matter structures, including the corpus callosum (Figs. 1B, 4E) and the anterior commissure (Fig. 1A). Moderate levels of PDE7A mRNA were seen in the cerebral peduncle (Fig. 5F) and in the interpeduncular nuclei (Fig. 5D), and low levels of expression in the middle cerebellar peduncle (Fig. 1F).

Moderate hybridization levels were also detected in the choroid plexus (Figs. 1C, 4A), the ependymal lining of the cerebral aqueduct (Fig. 5B). A strong hybridization signal was seen in the lateral ventricle (Fig. 1B).

Peripheral organs

PDE7A mRNA expression was analyzed in rat testis, thymus, spleen, liver, adrenal glands, and kidney. In testis, a high hybridization signal was observed in the interstices between the convoluted seminiferous tubules (Fig. 8A), corresponding to Leydig cells (Fig. 8B). PDE7A mRNA hybridization levels were high and presented a homogeneous distribution in the thymus lobules, with no differences between cortex and medulla (Fig. 8C).

In the spleen, PDE7A mRNA hybridization showed a patchy distribution, with much higher signals detected in the white pulp, or Malpighian bodies, than in the red pulp (Fig. 8D,E).

A gradient in the intensity of the hybridization signal was observed in the adrenal gland cortical layers (Fig. 8F). High hybridization levels were seen in the zona glomerulosa, decreasing toward the zona fasciculata and the zona reticularis. In the adrenal medulla, moderate hybridization levels for PDE7A mRNA were observed throughout.

The liver lobule presented low levels of PDE7A mRNA expression around the central vein (Fig. 8G). The signal detected was attributable to the liver cell plates located between the liver sinusoids.

In kidney, the medulla (Fig. 8H) and the collecting tubules (Fig. 8I) exhibited very high hybridization signal for PDE7A mRNA, especially in the papillary ducts of Bellini (Fig. 8J). PDE7A transcripts were also present at high levels in the epithelium of the renal papilla (Fig. 8J). In the cortex, intermediate levels were observed in the medullary rays (Fig. 8H).

Distribution of PDE7A1 and PDE7A2 splice variants by RT-PCR

Experiments were carried out to attempt to amplify by PCR the two splice variants PDE7A1 and PDE7A2 from RNA isolated from nine rat brain areas: olfactory bulb, cortex, midbrain, thalamus, hippocampus, striatum, cerebellum, brainstem, and spinal cord. PCR products of the expected size for PDE7A1 and PDE7A2 were identified in some brain areas, shown in Figure 9. PDE7A1 was amplified in midbrain, thalamus, and striatum. Less intense bands were observed in the cerebellum, cortex, and brainstem. A very weak band could be appreciated in the hippocampus. However, no bands could be amplified in the RNAs from olfactory bulb and spinal cord, although PDE7A1 could be amplified when higher RNA concentrations from olfactory bulb were used in the reaction (data not shown). PDE7A2 was clearly amplified in spinal cord, cortex, olfactory bulb, thalamus, hippocampus, and brainstem. Weak bands were obtained in cerebellum and midbrain, whereas no band could be observed in the striatum.

DISCUSSION

We examined the cellular and regional distribution of PDE7A in the rat brain and several peripheral organs by using an oligonucleotide complementary to the mRNA coding for this isozyme. Our results show that PDE7A mRNA is widely and heterogeneously distributed in the brain and expressed in both neuronal and nonneuronal cells. In peripheral organs, the hybridization signal presents a heterogeneous cellular distribution with the exception of the thymus, where the expression of PDE7A mRNA is homogeneous. A further degree of complexity is found when the distribution of the two reported spliced forms of this mRNA is examined by RT-PCR. While cortex, midbrain, brainstem, thalamus, hippocampus, and cerebellum appear to express both forms, only PDE7A1 mRNA is amplified from the striatum and PDE7A2 in spinal cord and olfactory bulb.

To our knowledge, this is the first detailed report of the regional and cellular distribution of PDE7A mRNA in the rat. Previous studies have only partially addressed this issue using RT-PCR and in situ hybridization histochemistry (Hoffmann et al., 1998). The wide

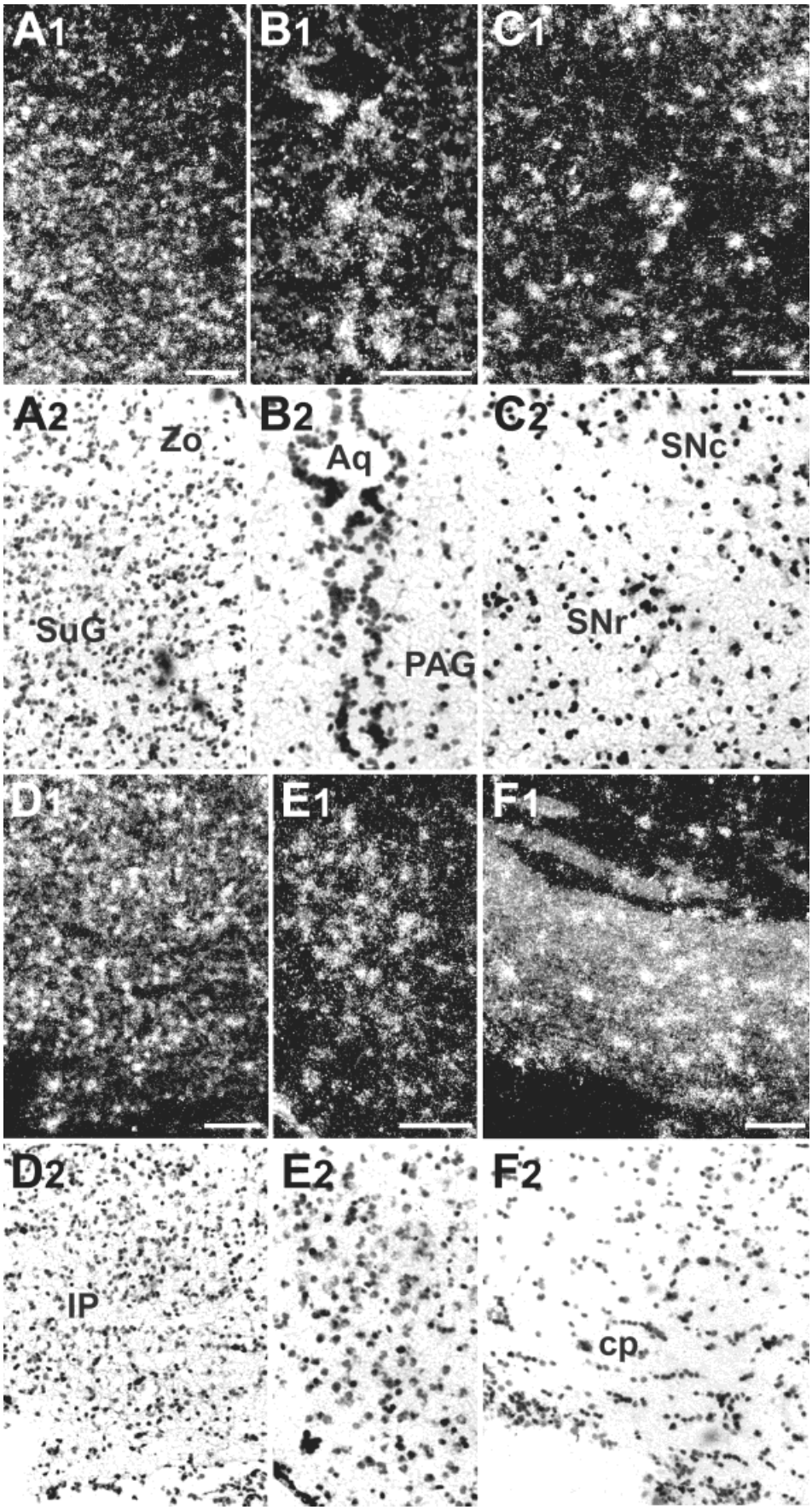

Fig. 5. Cellular localization of PDE7A mRNA in the superior colliculus (**A**), aqueduct (**B**), substantia nigra (**C**), interpeduncular nuclei (**D**), posteromedial cortical amygdaloid nucleus (**E**), and cerebral peduncle (**F**). Dark-field photomicrographs from emulsion-dipped hybridized sections (**A1–F1**). **A2–F2**: The same sections stained with cresyl violet. Bar = 0.1 mm. Aqueduct (Aq), cerebral peduncle (cp), interpeduncular nuclei (IP), periaqueductal grey (PAG), substantia nigra pars compacta (SNc) and pars reticulata (SNr), superficial gray layer of superior colliculus (SuG), zonal layer of superior colliculus (Zo).

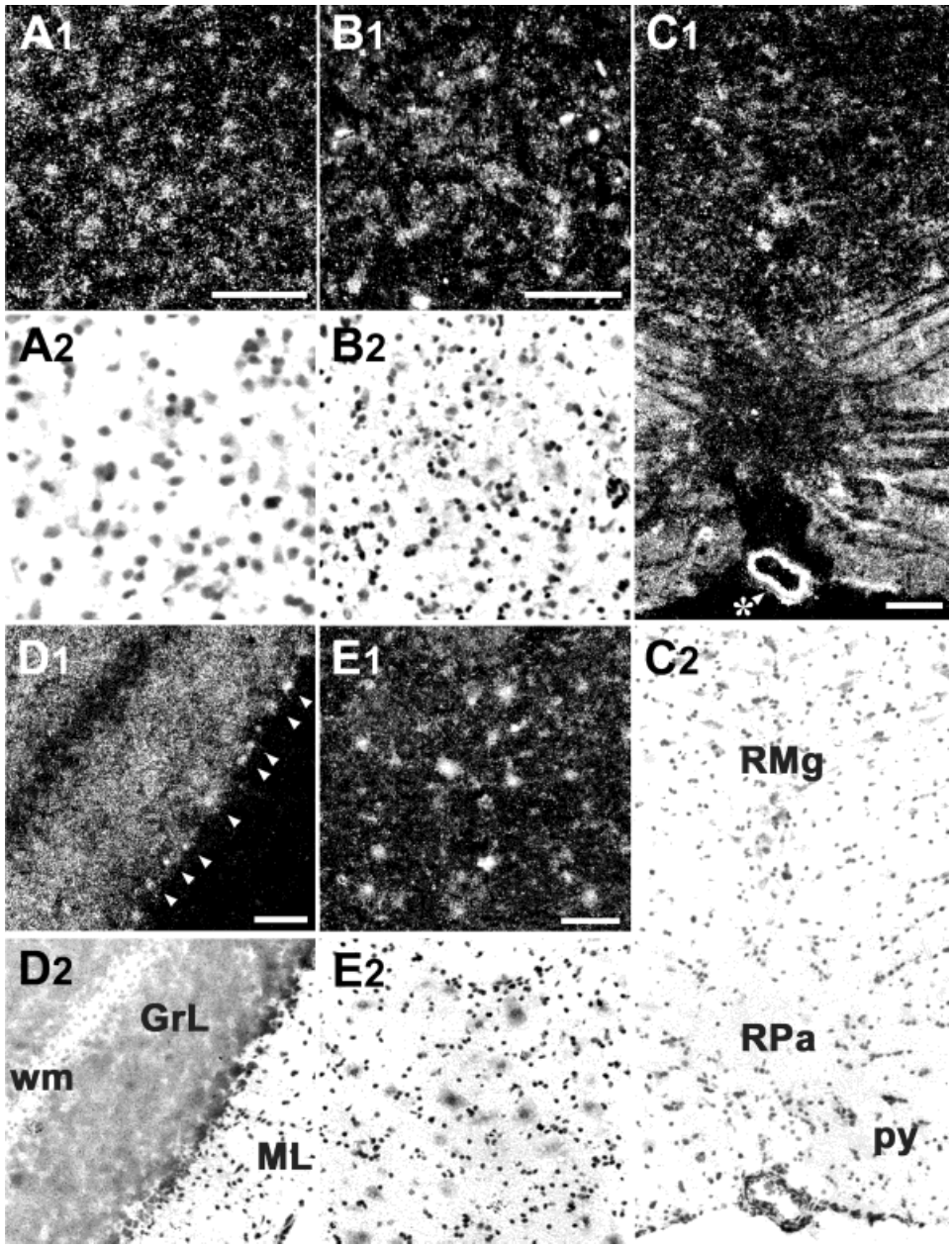

Fig. 6. Expression of PDE7A mRNA in the dorsal (**A**) and median (**B**) raphe nuclei, raphe magnus and pallidus nuclei (**C**), cerebellum (**D**), and nucleus of the solitary tract (**E**). Arrows in **D1** indicate labeled Purkinje cells. Asterisk in **C1** marks tissue light in the basilar artery. **A1–E1**: Photomicrographs from emulsion autoradiograms, obtained with dark-field illumination. **A2–E2**: Bright-field photomicrographs from the same sections stained with cresyl violet. Bar = 0.1 mm. Granular layer (GrL) and molecular layer (ML) of the cerebellum, pyramidal tract (py), raphe magnus nucleus (RMg), raphe pallidus nucleus (RPa), white matter (wm).

distribution of PDE7A mRNA suggests that this enzyme may be involved in regulating cAMP levels in cells with a wide range of functions.

Distribution of PDE7A mRNA in brain and peripheral organs: Comparison with ther phosphodiesterases

When PDE7A mRNA localization is compared with that of the other four members of cAMP-dependent PDE4 family (Pérez-Torres et al., 2001), some overlap of the expression pattern can be observed. The presence in the rat brain of other cAMP-specific phosphodiesterases, such as PDE7B (Hetman et al., 2000; Sasaki et al., 2000), PDE8 (Fisher et al., 1998; Hayashi et al., 1998), and the cAMP- and cGMP-specific PDE10A (Loughney et al., 1999) has been reported, in all cases by Northern blot analysis. The recently described cAMP- and cGMP-specific PDE11A (Fawcett et al., 2000), however, has not been found to be expressed in brain.

In this study we also detected PDE7A mRNA expression in the Leydig cells, where the endocrine function of the testis takes place. Since the synthesis of testosterone is mediated by cAMP, PDE7A could conceivably play a role in the regulation of this process.

In the spleen, the white pulp, made up of diffuse and nodular lymphoid tissue, presents high levels of PDE7A mRNA. The red pulp, formed by the venous sinuses, in contrast shows low levels. PDE7A mRNA is homogeneously distributed in the thymus, in both medullar and cortical areas. The lymphocytes that do not degenerate within the organ go on to differentiate in the peripheral lymphoid organs into T lymphocytes. In

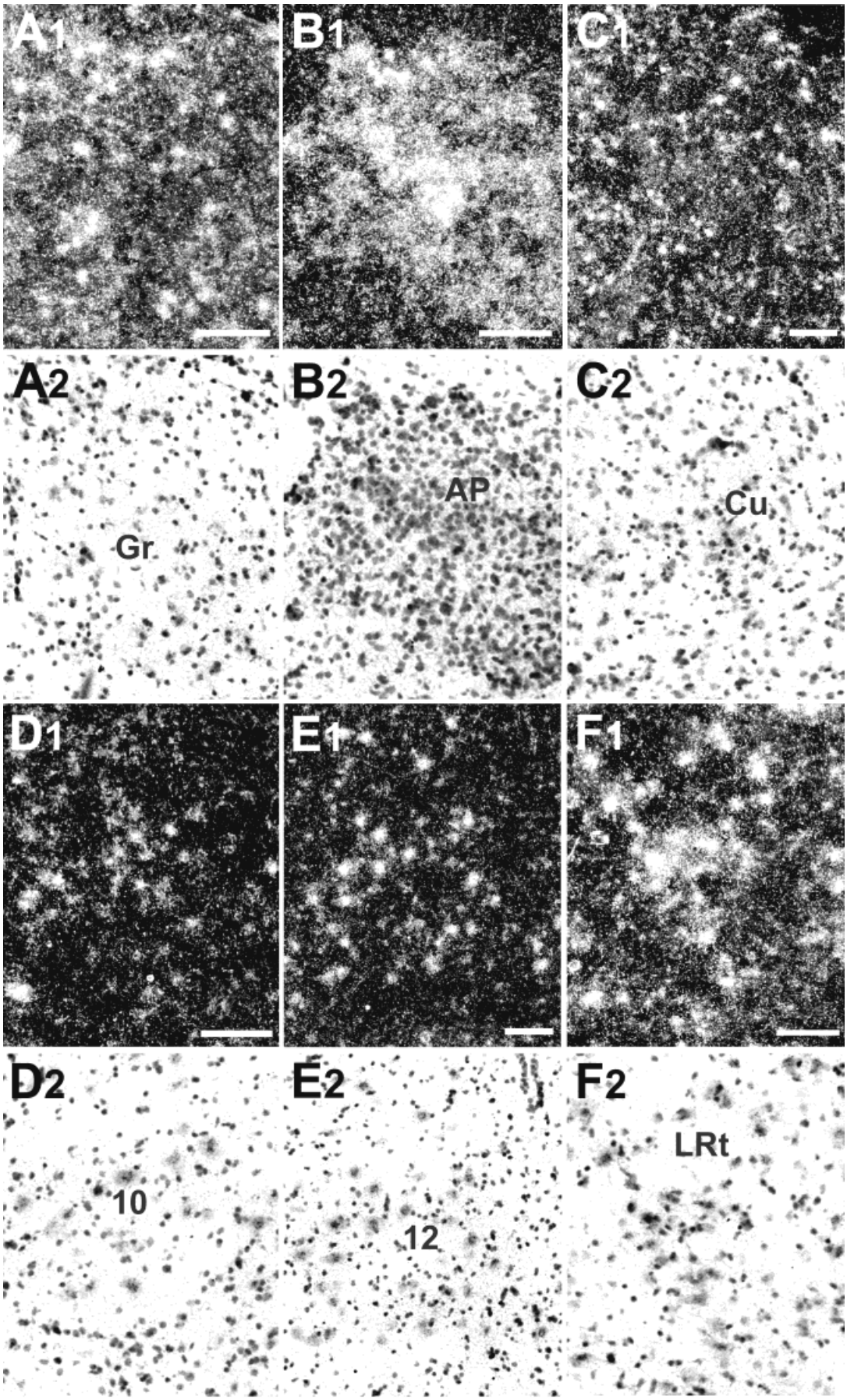

Fig. 7. Distribution of cells expressing PDE7A mRNA in the gracile nucleus (Gr) (**A**), area postrema (AP) (**B**), cuneate nuclei (Cu) (**C**), dorsal motor nucleus of vagus (10) (**D**), hypoglossal nucleus (12) (**E**), and lateroreticular nucleus (LRt) (**F**). Dark-field photomicrographs from emulsion-dipped tissue (**A1–F1**). **A2–F2**: The same sections stained with cresyl violet. Bars = 0.1 mm.

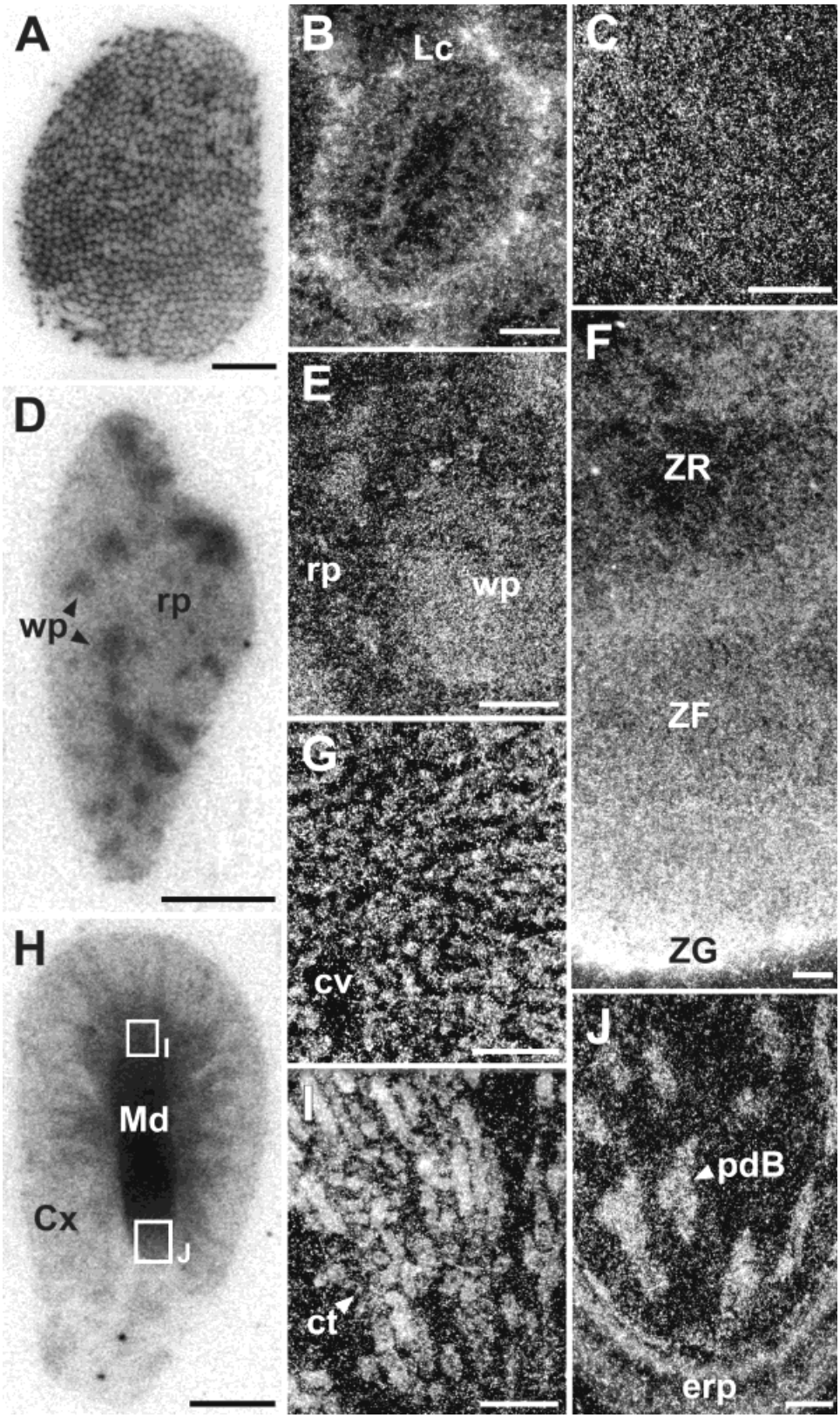

Fig. 8. Distribution of PDE7A mRNA in peripheral organs: testis (**A,B**) where it is expressed in Leydig cells, thymus (**C**), spleen (**D,E**), having a prominent expression in white pulp, adrenal glands (**F**) mainly expressed in the zona glomerulosa, liver (**G**), and kidney (**H**) being clearly present in the collecting ducts (**I**) and papillary ducts of Bellini (**J**). **A,D,H**: Film autoradiograms. **B,C,E–G,I,J**: Photomicrographs from emulsion autoradiograms, obtained with dark-field illumination. Bars = 4 mm (**A,D,H**) and 0.1 mm (**B,C,E–G,I,J**). Collecting tubules (ct), central vein (cv), cortex (Cx), epithelium of the renal papilla (erp), Leydig cells (Lc), medulla (Md), papillary ducts of Bellini (pdB), red pulp (rp), white pulp (wp), zona fasciculata (ZF), zona glomerulosa (ZG), zona reticularis (ZR).

fact, PDE7A expression has been described in two human T-cell lines (Bloom and Beavo, 1996) and in human $CD4^+$ and $CD8^+$ T-lymphocytes (Giembycz et al., 1996). It has also been recently demonstrated that PDE7 induction and the consequent suppression of cAMP-dependent protein kinase A (PKA) activity is required for T-cell activation (Li et al., 1999). All these data indicate that PDE7A may be a good target for the

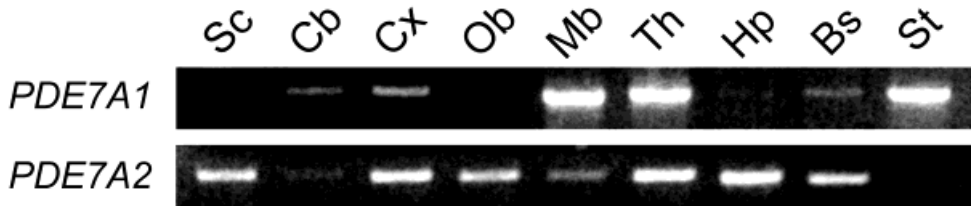

Fig. 9. RT-PCR analysis of the expression of PDE7A isoforms in nine rat brain regions. PDE7A1 mRNA was mainly enriched in midbrain, thalamus, and striatum, whereas it was not detected in spinal cord. PDE7A2 mRNA was present in spinal cord, cortex, olfactory bulb, thalamus, hippocampal formation, and brainstem, and was not amplified in striatum. Brainstem (Bs), cerebellum (Cb), cortex (Cx), hippocampal formation (Hp), midbrain (Mb), olfactory bulb (Ob), spinal cord (Sc), striatum (St), thalamus (Th).

development of selective inhibitors of T-cell response. The presence of PDE7 mRNA in B lymphocytes has also been demonstrated by RT-PCR (Gantner et al., 1998). This is of particular interest, since a variety of B-cell responses are modulated by cAMP (Holte et al., 1988).

A gradient of expression for PDE7A mRNA has been detected in the adrenal cortical layers. The highest expression was observed in the zona glomerulosa, decreasing in the zona fasciculata, and with low levels in the zona reticularis, where it could be involved in the regulation of hormone secretion.

In the adrenal medulla, intermediate levels of PDE7A mRNA are found. The catecholamines epinephrine and norepinephrine are contained in the cells of the medulla. Unlike the steroid hormones of the cortex, they accumulate at high concentrations in the cells, being involved in blood pressure, heart rate, and cardiac output. A cAMP-dependent basal catecholamine release has been described (Mazzocchi et al., 1999) where cAMP-specific PDE7A could play a role.

Several cyclic nucleotide phosphodiesterases have been described in the kidney (Dousa, 1999), where they participate in different regulatory pathways. We found that the PDE7A hybridization signals are present in the collecting tubules and absent in the nephron structures. Thus, intermediate levels of PDE7A mRNA are seen in the medullary rays and in the papillary ducts of Bellini. Higher activity of PDE4 and, to a lesser degree PDE3, have been proposed as responsible for nephrogenic diabetes insipidus (NDI) by the use of specific inhibitors (Takeda et al., 1991). The lack of specific PDE7 inhibitors in those studies and the presence of PDE7A mRNA described here suggests its possible implication in the regulation of cAMP levels in the collecting ducts.

PDE7A functions

The lack of specific inhibitors has prevented an analysis of the correlation between the localization of PDE7A enzyme and the functions mediated by this (these) enzyme(s). In the case of the PDE4 family the availability of several inhibitors, particularly rolipram, has made possible an extensive examination of the functions associated with the regulation of cAMP levels by the PDE4 enzyme family (Bach et al., 1999; Barad et al., 1998; Bertolino et al., 1988; Heaslip and Evans, 1995; Hebenstreit et al., 1989; Takahashi et al., 1999). The K_D of PDE7 for cAMP is about 10-fold higher than that of PDE4, suggesting a role for PDE7 when low levels of substrate are present. It will be interesting to see, once PDE7 inhibitors are available (Martínez et al., 2000), if they also produce behavioral, cellular, or molecular effects similar to rolipram.

CONCLUSIONS

PDE7A mRNA is present not only in several neuronal populations, but also in nonneuronal populations in brain and peripheral tissues. In the brain, splice forms of this mRNA show clear regional differences. These results provide information for more selective studies on the functions regulated by this enzyme, once other tools such as antibodies and selective inhibitors are available.

ACKNOWLEDGMENT

This work was supported by grants from Fundació La Marató de TV3 (1017/97), and CICYT (SAF1999-0123 and 2FD97-0395). X.M. is a recipient of a fellowship from CIRIT (Centre de Referència of the Generalitat de Catalunya) and S.P.-T. from CIRIT (Generalitat de Catalunya).

REFERENCES

Bach ME, Barad M, Son H, Zhuo M, Lu YF, Shih R, Mansuy I, Hawkins RD, Kandel ER. 1999. Age-related defects in spatial memory are correlated with defects in the late phase of hippocampal long-term potentiation in vitro and are attenuated drugs that enhance the cAMP signaling. Proc Natl Acad Sci USA 96:5280–5285.

Barad M, Bourtchouladze R, Winder DG, Golan H, Kandel E. 1998. Rolipram, a type IV-specific phosphodiesterase inhibitor, facilitates the establishment of long-lasting long-term potentiation and improves memory. Proc Natl Acad Sci USA 95:15020–15025.

Bertolino A, Crippa D, di Dio S, Fichte K, Musmeci G, Porro V, Rapisarda V, Sastre-y-Hernandez M, Schratzer M. 1988. Rolipram versus imipramine in inpatients with major, "minor" or atypical depressive disorder: a double-blind double-dummy study aimed at testing a novel therapeutic approach. Int Clin Psychopharmacol 3:245–253.

Bloom TJ, Beavo JA. 1996. Identification and tissue-specific expression of PDE7 phosphodiesterase splice variants. Proc Natl Acad Sci USA 93:14188–14192.

Conti M, Jin SL. 1999. The molecular biology of cyclic nucleotide phosphodiesterases. Prog Nucleic Acid Res Mol Biol 63:1–38.

Cherry JA, Davis RL. 1999. Cyclic AMP phosphodiesterases are localized in regions of the mouse brain associated with reinforcement, movement, and affect. J Comp Neurol 407:287–301.

Chomczynski P, Sacchi N. 1987. Single-step method of RNA isolation by acid guanidinium thiocyanate-phenol-chloroform extraction. Anal Biochem 162:156–159.

Dousa TP. 1999. Cyclic nucleotide phosphodiesterase isozymes in cell biology and pathophysiology of the kidney. Kidney Int 55:29–62.
Fawcett L, Baxendale R, Stacey P, McGrouther C, Harrow I, Soderling S, Hetman J, Beavo JA, Phillips SC. 2000. Molecular cloning and characterization of a distinct human phosphodiesterase gene family: PDE11A. Proc Natl Acad Sci USA 97:3702–3707.
Fisher DA, Smith JF, Pillar JS, St Denis SH, Cheng JB. 1998. Isolation and characterization of PDE8A, a novel human cAMP-specific phosphodiesterase. Biochem Biophys Res Commun 246:570–577.
Gantner F, Gotz C, Gekeler V, Schudt C, Wendel A, Hatzelmann A. 1998. Phosphodiesterase profile of human B lymphocytes from normal and atopic donors and the effects of PDE inhibition on B cell proliferation. Br J Pharmacol 123:1031–1038.
Genain CP, Roberts T, Davis RL, Nguyen MH, Uccelli A, Faulds D, Li Y, Hedgpeth J, Hauser SL. 1995. Prevention of autoimmune demyelination in non-human primates by a cAMP-specific phosphodiesterase inhibitor. Proc Natl Acad Sci USA 92:3601–3605.
Giembycz MA, Corrigan CJ, Seybold J, Newton R, Barnes PJ. 1996. Identification of cyclic AMP phosphodiesterases 3, 4 and 7 in human $CD4^+$ and $CD8^+$ T-lymphocytes: role in regulating proliferation and the biosynthesis of interleukin-2. Br J Pharmacol 118:1945–1958.
Goulding EH, Tibbs GR, Siegelbaum SA. 1994. Molecular mechanism of cyclic-nucleotide-gated channel activation. Nature 372:369–374.
Hayashi M, Matsushima K, Ohashi H, Tsunoda H, Murase S, Kawarada Y, Tanaka T. 1998. Molecular cloning and characterization of human PDE8B, a novel thyroid-specific isozyme of 3',5'-cyclic nucleotide phosphodiesterase. Biochem Biophys Res Commun 250: 751–756.
Heaslip RJ, Evans DY. 1995. Emetic, central nervous system, and pulmonary activities of rolipram in the dog. Eur J Pharmacol 286: 281–290.
Hebenstreit GF, Fellerer K, Fichte K, Fischer G, Geyer N, Meya U, Sastre-y-Hernandez M, Schony W, Schratzer M, Soukop W, Trampitsch E, Varosanec S, Zawada E, Zochling R. 1989. Rolipram in major depressive disorder: results of a double-blind comparative study with imipramine. Pharmacopsychiatry 22:156–160.
Hetman JM, Soderling SH, Glavas NA, Beavo JA. 2000. Cloning and characterization of PDE7B, a cAMP-specific phosphodiesterase. Proc Natl Acad Sci USA 97:472–476.
Hoffmann R, Abdel'Al S, Engels P. 1998. Differential distribution of rat PDE-7 mRNA in embryonic and adult rat brain. Cell Biochem Biophys 28:103–113.
Holte H, Torjesen P, Blomhof HK, Ruud E, Bjoro T, Pfeifer-Ohlsson S, Watt R, Funderud S, Godal T, Ohlsson R. 1988. Cyclic AMP has the ability to influence multiple events during B cell stimulation. Eur J Immunol 18:1359–1366.
Horowski R, Sastre-y-Hernandez M. 1985. Clinical effects of the neurotropic selective cAMP phosphodiesterase inhibitor rolipram in depressed patients: global evaluation of the preliminary reports. Curr Ther Res 38:23–29.
Houslay MD, Milligan G. 1997. Tailoring cAMP-signalling responses through isoform multiplicity. Trends Biochem Sci 22:217–224.
Houslay MD, Sullivan M, Bolger GB. 1998. The multienzyme PDE4 cyclic adenosine monophosphate-specific phosphodiesterase family: intracellular targeting, regulation, and selective inhibition by compounds exerting anti-inflammatory and antidepressant actions. Adv Pharmacol 44:225–342.
Hulley P, Hartikka J, Abdel'Al S, Engels P, Buerki HR, Wiederhold KH, Muller T, Kelly P, Lowe D, Lubbert H. 1995. Inhibitors of type IV phosphodiesterases reduce the toxicity of MPTP in substantia nigra neurons in vivo. Eur J Neurosci 7:2431–2440.
Kandel ER, Schwartz JH. 1982. Molecular biology of learning: modulation of transmitter release. Science 218:433–443.
Kato H, Araki T, Itoyama Y, Kogure K. 1995. Rolipram, a cyclic AMP-selective phosphodiesterase inhibitor, reduces neuronal damage following cerebral ischemia in the gerbil. Eur J Pharmacol 272:107–110.
Kaufman S. 1995. Tyrosine hydroxylase. Adv Enzymol Relat Areas Mol Biol 70:103–220.
Lalli E, Sassone-Corsi P. 1994. Signal transduction and gene regulation: the nuclear response to cAMP. J Biol Chem 269:17359–17362.
Li L, Yee C, Beavo JA. 1999. CD3 and CD28-dependent induction of PDE7 required for T cell activation. Science 283:848–851.
Loughney K, Snyder PB, Uher L, Rosman GJ, Ferguson K, Florio VA. 1999. Isolation and characterization of PDE10A, a novel human 3', 5'-cyclic nucleotide phosphodiesterase. Gene 234:109–117.
Martinez A, Castro A, Gil C, Miralpeix M, Segarra V, Domenech T, Beleta J, Palacios JM, Ryder H, Miro X, Bonet C, Casacuberta JM, Azorin F, Piña B, Puigdomenech P. 2000. Benzyl derivatives of 2,1,3-benzo-and benzothieno[3,2-a]thiadiazine 2,2-dioxides: first phosphodiesterase 7 inhibitors. J Med Chem 43:683–689.
Mazzocchi G, Andreis PG, De Caro R, Aragona F, Gottardo L, Nussdorfer GG. 1999. Cerebellin enhances in vitro secretory activity of human adrenal gland. J Clin Endocrinol Metab 84:632–635.
McGeer PL, McGeer EG. 1995. The inflammatory response system of brain: implications for therapy of Alzheimer and other neurodegenerative diseases. Brain Res Rev 21:195–218.
Michaeli T, Bloom TJ, Martins T, Loughney K, Ferguson K, Riggs M, Rodgers L, Beavo JA, Wigler M. 1993. Isolation and characterization of a previously undetected human cAMP phosphodiesterase by complementary of cAMP phosphodiesterase-deficient *Saccharomyces cerevisiae*. J Biol Chem 268:12925–12932.
Morimoto BH, Koshland DEJ. 1991. Identification of cyclic AMP as the response regulator for neurosecretory potentiation: a memory model system. Proc Natl Acad Sci USA 88:10835–10839.
Pérez-Torres S, Miró X, Palacios JM, Puigdomènech P, Mengod G. 2001. PDE4 isozymes expression in human brain examined by in situ hybridization histochemistry and rolipram binding sites. Comparison with monkey and rat brains. J Chem Neuroanat 20:349–374.
Sasaki T, Kotera J, Yuasa K, Omori K. 2000. Identification of human PDE7B, a cAMP-specific phosphodiesterase. Biochem Biophys Res Commun 271:575–583.
Soderling SH, Bayuga SJ, Beavo JA. 1998. Cloning and characterization of a cAMP-specific cyclic nucleotide phosphodiesterase. Proc Natl Acad Sci USA 95:8991–8996.
Takahashi M, Terwilliger R, Lane C, Mezes PS, Conti M, Duman RS. 1999. Chronic antidepressant administration increases the expression of cAMP-specific phosphodiesterase 4A and 4B isoforms. J Neurosci 19:610–618.
Takeda S, Lin CT, Morgano PG, McIntyre SJ, Dousa TP. 1991. High activity of low-Michaelis-Menten constant 3',5'-cyclic adenosine monophosphate-phosphodiesterase isozymes in renal inner medulla of mice with hereditary nephrogenic diabetes insipidus. Endocrinology 129:287–294.
Teixeira MM, Gristwood RW, Cooper N, Hellewell PG. 1997. Phosphodiesterase (PDE)4 inhibitors: anti-inflammatory drugs of the future? Trends Pharmacol Sci 18:164–171.
Tomiyama M, Palacios JM, Cortés R, Vilaró MT, Mengod G. 1997. Distribution of AMPA receptor subunit mRNAs in the human basal ganglia: an in situ hybridization study. Mol Brain Res 46:281–289.
Yamashita N, Hayashi A, Baba J, Sawa A. 1997. Rolipram, a phosphodiesterase-4-selective inhibitor, promotes the survival of cultured rat dopaminergic neurons. Jpn J Pharmacol 75:155–159.
Zagotta WN, Siegelbaum SA. 1996. Structure and function of cyclic nucleotide-gated channels. Annu Rev Neurosci 19:235–263.
Zhong Y, Wu CF. 1991. Altered synaptic plasticity in Drosophila memory mutants with a defective cyclic AMP cascade. Science 251:198–201.